''Partial pressures'' supported by granulometric classes in polydisperse granular media

Olivier Tsoungui, Denis Vallet, Jean-Claude Charmet, and Stéphane Roux
Laboratoire de Physique et Mécanique des Milieux Hétérogènes, CNRS URA No. 857, Ecole Supérieure de Physique et Chimie Industrielles de la Ville de Paris, 10 rue Vauquelin, 75231 Paris Cedex 05, France

(Received 3 July 1997; revised manuscript received 31 October 1997)

A packing of particles subjected to an œdometric compression displays a large distribution of interparticle contact forces. The latters are correlated with the particle size. Using the principle of virtual work, we relate the ''partial'' pressure supported by a granulometric class of particles to a purely geometrical problem, namely, the solid fraction of a polydisperse granular medium as a function of its granulometry. We apply in particular this result to the case of bimodal packings and we show that the partial pressure is larger for the small particles in three dimensions, whereas a size independence is predicted in two dimensions. Two- and three-dimensional numerical simulations confirm these results. [S1063-651X(98)07304-8]

PACS number(s): 83.70.Fn, 01.55.+b, 07.05.Fb, 46.10.+z

I. INTRODUCTION

Photoelastic visualizations of two-dimensional (2D) [1–3] and three-dimensional (3D) [4] granular systems provide striking evidence of the heterogeneous distribution of intergranular stresses in a granular system on a scale definitely larger than the typical particle size [5–7]. This motivated some recent works devoted to the analysis of the statistical distribution of interparticle forces [7–12]. Apart from this basic level of description, the statistical correlation of these forces in the medium still requires a detailed analysis. We present a step in this direction, from the analysis of the correlation between the force at a contact and the particle size.

It is of uttermost importance to have a faithful description of this geometrical organization for processes like particle fragmentation. Indeed, it is well known that a small amount of recycling of small particles in a crushing device leads to an increased efficiency of crushing. Although this question is directly related to the local stress distribution around the particle, no satisfactory understanding is yet available on this point and the recycling rate is based on empirical rules.

In this paper we are particularly interested by the local pressures supported by the particles within a polydisperse packing. One interesting question is how these local pressures depend on the grain sizes when external forces are applied. Assuming that each contact force is identical to all others, Helle *et al.* [13] used the principle of virtual work to determine the average contact force between identical spheres subjected to a remote pressure as a function of their mean coordination number, and relative density. From a similar principle, we develop a theoretical model [14] that relates the ''partial'' pressures supported by granulometric classes of particles to a purely geometrical problem, namely, the determination of the solid fraction as a function of the granulometry. As a side product, it allows us to deduce the mean normal force of one contact on a grain as a function of the external pressure and the mean coordination number.

In order to validate this theoretical model, two- and three-dimensional numerical simulations based on molecular dynamics (MD) method with elastic interactions between the grains have been performed for various combinations of grain sizes and granulometric class proportions. For a range of external pressures applied on each sample, we numerically determine the solid fraction, the coordination number, the mean normal force of one contact on a grain, and the partial pressures supported by the granulometric classes. We compare the theoretical prediction with these numerically determined results. The range of external pressures is chosen so that the density of the packing varies by about 6.5%.

In Sec. II, we introduce the theoretical model and we present the predicted results on the partial pressures in particular for bidisperse packings; in Sec. III, we briefly present the simulation method and we compare the numerical results with those of the theoretical model; in Sec. IV, we discuss the limits of the model.

II. THEORETICAL MODEL

A. Description

Let us consider a packing of N spherical or cylindrical grains with a statistical distribution, $f(x)$, such that $Nf(x)dx$ is the number of particles whose diameter lies in the range $[x,x+dx]$. The packing is supposed dense with a spatial homogeneous distribution of particles.

We introduce the mean particle volume $\overline{\nu}$,

$$\overline{\nu}=S_d\int_0^\infty x^d f(x)\,dx, \tag{1}$$

where S_d is the volume of a unit diameter sphere in d dimensions, i.e., $S_2=\pi/4$ and $S_3=\pi/6$.

We take an interest in the mean pressure (partial pressure), $\langle p(x)\rangle$, supported by a grain of diameter x when external forces are applied on the packing. $\langle p(x)\rangle$ is defined as the ratio of the sum of normal contact forces on the particles of diameter x, divided by their areas,

$$\langle p(x)\rangle=\frac{\left\langle \sum F_i n_i\right\rangle}{A_d x^{d-1}}, \tag{2}$$

where F_i is the contact force at point i, n_i the external normal at this point, and A_d the area of a unit diameter sphere in

d dimensions, $A_2=A_3=\pi$. Note that $A_d=2dS_d$. The sum between angular brackets is applied on all contacts i of a particle of diameter x, and the angular brackets represent an average on all such particles.

In order to have access to this partial pressure $\langle p(x)\rangle$, we use the principle of virtual work. Let us imagine an infinitesimal virtual transformation such that the $N\delta f(x)$ particles of diameter x are dilated to a diameter $x+\delta x$. The internal virtual work δW_i of the contact forces on these particles is expressed as

$$\delta W_i=S_d N\delta f(x)\langle p(x)\rangle x^{d-1}\delta x. \tag{3}$$

In this transformation, the global packing volume expands by δV and the work δW_e of the external pressure P_{ext} is given by

$$\delta W_e=P_{\mathrm{ext}}\delta V. \tag{4}$$

The packing volume is

$$V=\frac{N\overline{\nu}}{c}, \tag{5}$$

where c is the density of the packing. We introduce here an essential hypothesis: the solid fraction is assumed to be a known functional of the granulometric distribution,

$$c=\mathcal{C}[f]. \tag{6}$$

Thus the virtual transformation previously introduced leads to a variation δc of density obtained from the above functional. We do not present here any new results on the density calculation but rather refer to previous studies of the literature [15–17].

By differentiation, we obtain the global volume variation,

$$\delta V=\frac{N\overline{\nu}}{c}\left(\frac{\delta\overline{\nu}(x)}{\overline{\nu}}-\frac{\delta c}{c}\right), \tag{7}$$

where

$$\delta\overline{\nu}(x)=dS_d x^{d-1}\delta x\,\delta f. \tag{8}$$

The principle of virtual work allows us to write the equality $\delta W_i=\delta W_e$ and we obtain the following key result:

$$\frac{\langle p(x)\rangle}{P_{\mathrm{ext}}}=\frac{1}{c}\left(1-\frac{\overline{\nu}}{c}\,\frac{\delta c}{\delta\overline{\nu}(x)}\right), \tag{9}$$

where the left-hand side (lhs) contains the partial pressure we wanted to compute whereas the right-hand side (rhs) is a purely geometrical quantity.

From this general result, we can easily deduce the mean normal force $\langle F_n\rangle$ of one contact applied on a grain of the packing,

$$\langle F_n\rangle=\frac{A_d\langle x^{d-1}\rangle P_{\mathrm{ext}}}{\overline{n}c}\beta, \tag{10}$$

where $\overline{n}$ is the mean coordination number and

$$\beta=\int_0^\infty\left(1-\frac{\overline{\nu}}{c}\,\frac{\delta c}{\delta\overline{\nu}(x)}\right)f(x)dx. \tag{11}$$

Note that, for the monodisperse packings ($f=0$ or $f=1$), we have $\delta c/\delta\overline{\nu}(x)=0$ and $\beta=1$; thus we recover the relation proposed by Helle *et al.* [13],

$$\langle F_n\rangle=\frac{\pi\langle x^{d-1}\rangle P_{\mathrm{ext}}}{\overline{n}c}. \tag{12}$$

These results relate the partial pressure supported by a granulometric class of particles to a purely geometrical problem, i.e., the change of solid fraction as a function of an infinitesimal transformation.

B. Particular case of a bimodal distribution

In order to illustrate the preceding results, we consider the case of a bimodal distribution where x only takes two values x_1 and x_2. We define $\alpha\equiv x_1/x_2$ with the convention $\alpha<1$.

Let $f_1=f$ the numerical proportion of small grains (diameter x_1), and therefore $f_2=1-f$ the proportion of large grains. In the present case, the solid fraction is defined as a function of the size ratio α and the numerical proportion f,

$$c=\psi(f,\alpha), \tag{13}$$

i.e., c depends only of size ratio and not absolute sizes. Hence, the application of preceding results on the partial pressures leads to the following expressions,

$$\frac{\langle p(x_1)\rangle}{P_{\mathrm{ext}}}=\frac{1}{c}\left(1-\frac{\alpha\overline{\nu}}{cdS_d x_1^d f}\,\frac{\partial\psi}{\partial\alpha}\right),$$

$$\frac{\langle p(x_2)\rangle}{P_{\mathrm{ext}}}=\frac{1}{c}\left(1+\frac{\alpha\overline{\nu}}{cdS_d x_2^d(1-f)}\,\frac{\partial\psi}{\partial\alpha}\right), \tag{14}$$

and

$$\beta=1+\frac{\alpha(\alpha^d-1)[f+(1-f)\alpha^d]}{d}\,\frac{\partial\log\psi}{\partial\alpha}. \tag{15}$$

These expressions can be simplified when we introduce the volume fractions $\xi=fS_d x_1^d/\overline{\nu}$ for the small grains and $(1-\xi)$ for the large ones.

From now on, we must argue differently depending on the spatial dimension d of the system.

As a matter of fact, the density of three-dimensional bimodal systems depends crucially of the size ratio and the numerical proportion of each granulometric class. Given α, the density as a function of the proportion f generally displays a sharp maximum for an optimal proportion $f^*(\alpha)$ with a kink near of this maximum. Decreasing the ratio α, this maximum increases (recall that $\alpha<1$ conventionally). This behavior is bounded by $\alpha>\alpha_c$ where $\alpha_c\approx 1/6$ is the critical ratio above which the small grains can fit inside the neck formed by three large grains in contact. In this case, a *segregation* takes place when the proportion f becomes less than the minimum required for filling the pore space of the large particles. Thus, as long as $\alpha>\alpha_c$, $\partial\psi/\partial\alpha$ is negative and the parameter $\beta>1$. We deduce that [see Eq. (14)] the smaller grains support a higher pressure than the larger ones in three dimensions.

In two dimensions, the situation is very different. Experimental results [17,18] provide evidence for a quasiconstant density as a function of the ratio α and the composition f. Therefore $\partial\psi/\partial\alpha\approx 0$ and $\beta\to 1$, from what we deduce that the partial pressure are equal for both types of particles, i.e., $\langle p(x_1)\rangle = \langle p(x_2)\rangle = P_{\text{ext}}/c$.

C. Application using Ouchiyama-Tanaka model

Ouchiyama and Tanaka have developed a purely theoretical model predicting the density of three-dimensional polydisperse granular media as a function of the statistical distribution of particle size, $f(x)$. Being general, this model can be used to the particular case of a bimodal distribution. The principle of this model is based on a geometrical self-consistent computation. It provides a good approximation as long as there is no *macropore* — i.e., pore spaces whose sizes are larger than the mean particle diameter $\langle x\rangle$ — in the packing. The hypothesis and calculations are detailed in the original reference [16].

We use this model to predict the evolution of partial pressures as a function of the granulometry. In the particular case of a bimodal distribution the solid fraction is given by

$$c=\frac{f\overline{x_1}^3+(1-f)\overline{x_2}^3}{(1-f)(\overline{x_2}-1)^3+(1/\eta)[f(\overline{x_1}+1)^3+(1-f)[(\overline{x_2}+1)^3-(\overline{x_2}-1)^3]]} \tag{16}$$

with

$$\eta=1+\frac{4}{13}(8c_o-1)\frac{f(\overline{x_1}+1)^2[1-\frac{3}{8}\,1/(\overline{x_1}+1)]+(1-f)(\overline{x_2}+1)^2[1-\frac{3}{8}\,1/(\overline{x_2}+1)]}{f\overline{x_1}^3+(1-f)[\overline{x_2}^3-(\overline{x_2}-1)^3]}, \tag{17}$$

where c_o is the density of a random monodisperse packing in three dimensions, and

$$\overline{x_1}=\frac{x_1}{\langle x\rangle}=\frac{\alpha}{\alpha f+(1-f)},$$

$$\overline{x_2}=\frac{x_2}{\langle x\rangle}=\frac{1}{\alpha f+(1-f)}. \tag{18}$$

From this model, the density variation $\partial\psi/\partial\alpha$ and the parameter β appearing, respectively, in Eqs. (14) and (15) can be found using Eqs. (16) and (17) and are given in Appendix A. Given α, this model leads to the theoretical determination of the partial pressures $\langle p(x_1)\rangle/P_{\text{ext}}$ and $\langle p(x_2)\rangle/P_{\text{ext}}$ as a function of the numerical proportion f.

Figure 1 shows an example of the predicted partial pressures in a packing combining our model with the Ouchiyama-Tanaka density prediction. Given $\alpha=1/3$ and $c_0=0.64$, this figure shows the variations of the density c, the partial pressures $\langle p(x_1)\rangle/P_{\text{ext}}$ and $\langle p(x_2)\rangle/P_{\text{ext}}$, and the parameters β and $-\partial\psi/\partial\alpha$ as a function of volume fraction ξ of small grains.

We note in this figure that the solid fraction presents a smooth maximum for a small particle volume fraction close to 0.2, but a rather small overall variation. A similar shape albeit with larger variations is obtained for the derivative of this density with respect to α. The relative partial pressures decrease significantly for a small volume fraction ξ before reaching a plateau value for ξ larger than 0.2 and 0.5 for $\langle p(x_2)\rangle$ and $\langle p(x_1)\rangle$, respectively. This plateau can be understood as resulting from the weak sensitivity of the density on the small particle volume fraction.

III. NUMERICAL SIMULATIONS

A. Simulation method

We have partially checked these theoretical predictions on the bimodal packings of grains under an œdometric compression, using numerical simulations.

The computer simulations are performed using a molecular dynamics (MD) algorithm [19,20]. A detailed description of the MD method can be found in the literature [21,22]. We specify a model for the contact forces between grains including dry friction as detailed below. We use a fifth order predictor-corrector algorithm for the integration of the Newtonian equations of motion, for the velocity and rotation of each particle. A simple disk or sphere geometry was assumed in two and three dimensions, respectively.

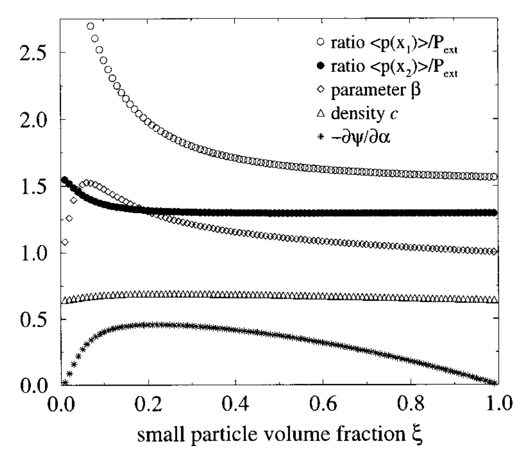

FIG. 1. Variations of the density c (△), the partial pressures $\langle p(x_1)\rangle/P_{\text{ext}}$ (○) and $\langle p(x_2)\rangle/P_{\text{ext}}$ (●), and the parameters β (◇) and $-\partial\psi/\partial\alpha$ (*) as a function of the volume fraction ξ of small grains as computed from the Ouchiyama-Tanaka model.

TABLE I. Numerical proportion f, size ratio α, mean coordination number $\overline{n}$, and solid fraction c in our samples A, B, C, D, E, and F before the reloading of the system ($P_{\mathrm{ext}} \approx 0$).

Sample (dimension)	f	α	$\overline{n}$	c
$A(d=2)$	72.9%	0.40	3.71	0.839
$B(d=2)$	69.2%	0.60	3.64	0.828
$C(d=2)$	85.5%	0.40	3.53	0.834
$D(d=3)$	88.0%	0.50	6.47	0.660
$E(d=3)$	94.9%	0.50	6.53	0.652
$F(d=3)$	96.4%	0.33	6.48	0.675

In MD simulations contact forces are at play only when particles overlap. For two grains i and j of respective diameter x_i and x_j in contact, we assume the normal repulsive contact force $|F_{\mathrm{el},ij}|$ due to the elastic deformation as directly proportional to the overlap δ_{ij} between two grains as

$$|F_{\mathrm{el},ij}| = Y X_n \delta_{ij}, \tag{19}$$

where $X_n = x_i x_j/(x_i + x_j)$ is the reduced diameter and Y is the Young modulus and which is chosen large enough so that the overlap is always a small fraction of the grain diameter.

The elastic deformation of the particles is assumed to be supplemented by a *viscous* damping force $F_{\mathrm{diss},ij}$ (related to the coefficient of restitution), which is chosen as

$$F_{\mathrm{diss},ij} = -m_n \gamma_n v_n, \tag{20}$$

where the reduced mass $m_n = m_i m_j/(m_i + m_j)$, γ_n is a phenomenological damping constant, and v_n the normal relative velocity between two particles. Thus the normal force is given as $F_{n,ij} = F_{\mathrm{el},ij} + F_{\mathrm{diss},ij}$.

Tangential (frictional) force $F_{\mathrm{friction},ij}$ is taken to be proportional to the extension of a tangential spring k_t as long as the magnitude of that spring force does not exceed the friction coefficient μ times the normal force. Above this threshold, a Coulomb friction law is invoked, and the tangential force remains constant at the value

$$F_{\mathrm{friction},ij} = -\mathrm{sgn}(\delta s)\min(k_t \delta s, \mu F_{n,ij}), \tag{21}$$

where δs is the shear displacement integrated over the entire contact time. In the simulations performed for this study, the coefficient of interparticle friction was chosen at a fixed value of $\mu = 0.3$. We also included a shear dynamic friction force, which in its simplest form can be chosen as

$$F_{\mathrm{shear},ij} = -m_n \gamma_t v_t, \tag{22}$$

where γ_t is the shear dynamic friction coefficient and v_t is the tangential relative velocity between the two particles. This force acts as a viscous damping on the absolute rotational velocities of the particles.

This program has been used to simulate the quasistatic evolution of an assembly. The simulated experiments were performed on packings of 700 disks in two dimensions and 1000 spheres in three dimensions. All these packings have a bimodal size distribution. Six samples of various combinations of grain sizes and granulometric class proportions are presented in Table I.

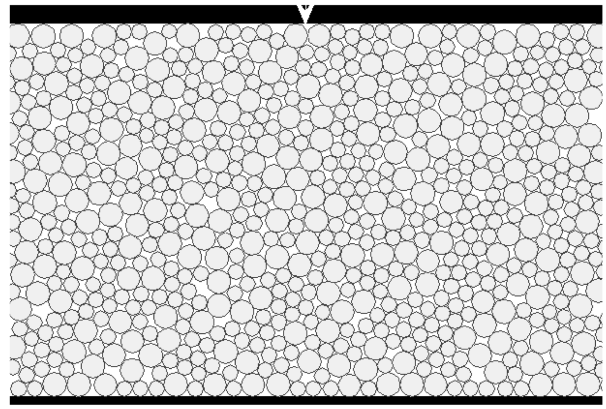

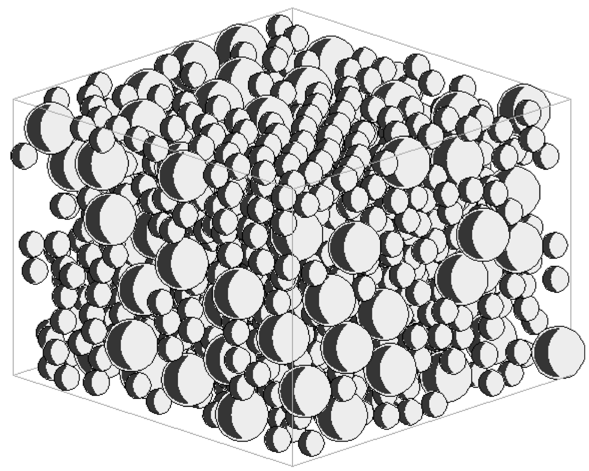

FIG. 2. Geometry of the two-dimensional packing (a) and the three-dimensional packing (b) used in the numerical simulations. Lateral boundary conditions are periodic.

Disks (or spheres) are enclosed by a fixed bottom plane and a top horizontal plane where the vertical displacement is imposed. Lateral boundary conditions are periodic, and thus the macroscopic strain is simply a uniaxial compression (œdometric compression). Figures 2(a) and 2(b) show, respectively, the two- and three-dimensional simulation geometry. This geometry guarantees the absence of lateral friction.

The construction of the packings takes place under gravity and we add a small random perturbation on the radii to avoid crystallization. We make sure that the constructed packings are dense with a spatial homogeneous distribution of particles. A first external pressure P_{ext} is applied on the system to achieve the consolidation phase. After unloading the system, we again apply a progressive load on top of the sample and we measure the density, the coordination number, the mean normal contact force, and the partial pressures supported by the two granulometric classes. Table I shows the quantities of the mean coordination number and the solid fraction inside each sample before the reloading of the system ($P_{\mathrm{ext}} \approx 0$). In order to preserve particle shapes, we have only retained the results with low values of global strain.

B. Numerical results

1. Two-dimensional packings

We first present the results obtained in two-dimensional samples. Figure 3 shows the products of partial pressures by

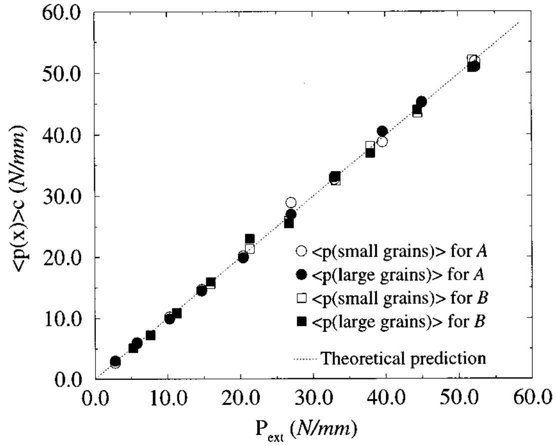

FIG. 3. Variations of the products of partial pressures by the solid fraction $\langle p_1\rangle c$ and $\langle p_2\rangle c$ as a function of external pressure P_{ext} applied on the granular samples A and B in two dimensions. The dotted line is the theoretical prediction.

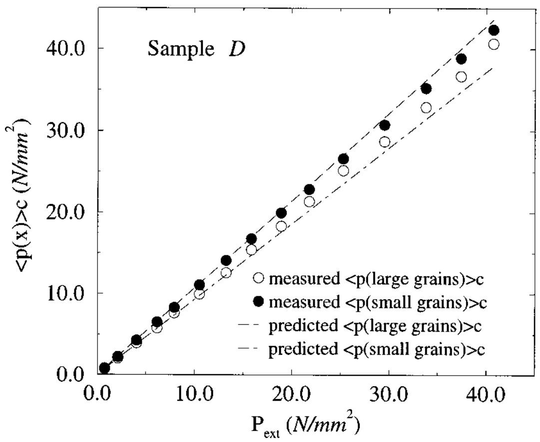

FIG. 5. Variations of the products of partial pressures by the solid fraction $\langle p_1\rangle c$ and $\langle p_2\rangle c$ as a function of external pressure P_{ext} applied on the granular sample D (three dimensions). The dotted lines are theoretical predictions using the Ouchiyama-Tanaka density model.

the density $\langle p(x_1)\rangle c$ and $\langle p(x_2)\rangle c$ as a function of external pressure P_{ext} applied on the granular samples A, B, and C. In this two-dimensional case we observe these quantities are approximately equal to the external pressure P_{ext}. As anticipated from the theoretical model in two dimensions we find $\partial\psi/\partial\alpha\approx 0$. Note that, however, the density of the packing varies by about 6.5% for the range of external pressures presented here.

We measure the mean normal force $\langle F_n\rangle$ contact on each granular system (all classes included). The previous theoretical analysis leads to

$$\langle F_n\rangle \equiv \frac{A_2\langle x\rangle P_{\mathrm{ext}}}{\overline{n}c}\beta, \tag{23}$$

where $A_2=\pi$ and $\beta\rightarrow 1$.

Figure 4 shows the variation of the product of the mean normal contact force $\langle F_n\rangle$ by the coordination number $\overline{n}$ divided by the mean particle perimeter $\langle F_n\rangle\overline{n}/\pi\langle x\rangle$ as a function of the ratio of external pressure P_{ext} on the density c. This figure shows that the slope of the regression through the data points tends to 1, $\beta\rightarrow 1$, in agreement with the theoretical prediction (dashed line in Fig. 4).

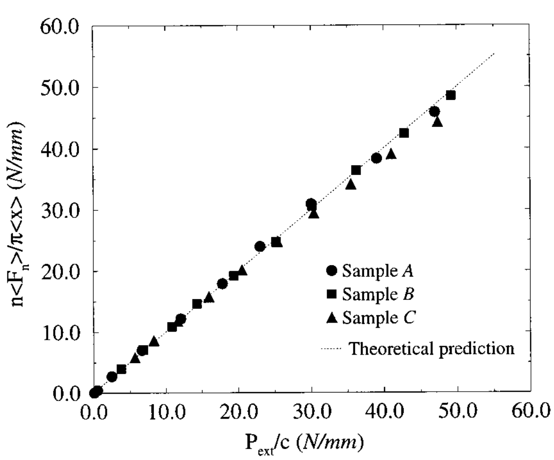

FIG. 4. Variations of the product of the mean normal force $\langle F_n\rangle$ contact by the coordination number $\overline{n}$ divided by the mean particle perimeter $\langle F_n\rangle\overline{n}/\pi\langle x\rangle$ as a function of the ratio of external pressure P_{ext} over the density c (two dimensions). The dotted line is the theoretical prediction using $\beta=1$.

These figures show that the theoretical predictions compare well with the numerically determined results. They confirm the independence of partial pressures with the particle size.

2. In three-dimensional packings

Similar analysis has been performed on three-dimensional packings. We numerically determined the density, the coordination number, the mean normal force at contact points, and the partial pressures supported by the granulometric classes. These quantities are compared to the theoretical predictions. In Fig. 5 we present the products of the partial pressures and the solid fraction $\langle p(x_1)\rangle c$ and $\langle p(x_2)\rangle c$ as a function of external pressure P_{ext} applied on the granular sample D. Contrary to two-dimensional packings (see Fig. 3) we observe that smaller grains support a higher pressure than the larger ones in three dimensions. This shows that the partial pressures increase with the external pressure P_{ext} as predicted in Eq. (14). The same observation holds as well for the other tested samples E and F. On this graph, we also display the prediction obtained from the Ouchiyama-Tanaka model, combined with our analysis. We note a good agreement for weak external pressures and a slight deviation for stronger external pressures. This discrepancy between the theoretical model and the data points may be a consequence of the geometrical variations within the samples during the compression, i.e., the establishment of new interparticle contacts between grains by local slidings and rollings, and the increase of the density. In fact, the combination of our model with the Ouchiyama-Tanaka density prediction does not allow one to account for these variations and considers the geometrical structure of the packing as invariant during the compression.

The mean normal force $\langle F_n\rangle$ was predicted to amount to

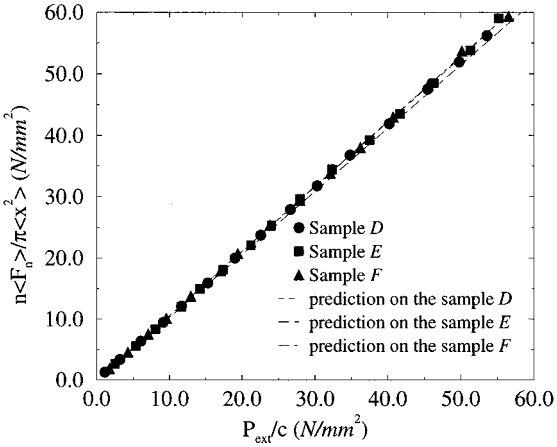

FIG. 6. Variations of the product of the mean normal force $\langle F_n \rangle$ contact by the coordination number $\overline{n}$ divided by the mean particle area $\langle F_n \rangle \overline{n}/\pi\langle x^2 \rangle$ as a function of the ratio of external pressure P_{ext} over the density c (three dimensions). The dotted lines are theoretical predictions using the Ouchiyama-Tanaka density model.

$$\frac{\langle F_n \rangle \overline{n}}{\pi\langle x^2 \rangle} = \frac{P_{\mathrm{ext}}}{c}\beta. \tag{24}$$

Figure 6 is a direct check of this equation, showing the graph of the lhs of the above equation as a function of the ratio of external pressure on the density. We first observe that the graph is indeed linear, and second, from a global point of view, the slope β as predicted by the Ouchiyama-Tanaka model (shown as a dotted line on the graph) provides a good description of the numerical data points. In contrast to two-dimensional packings, β is always greater than 1 and displays a rather weak dependence on the particle size ratio and the geometrical variations during the compression.

IV. DISCUSSION

The limitation of our model is due to the hypothesis that the solid fraction of the piling is uniquely determined by the granulometry. This in fact can only be regarded as an approximation, since the granulometry alone does not suffice to determine a solid fraction. Indeed it is well known that under vibration, a given medium can be compacted by typically a few percent under optimal conditions. Therefore the mentioned functional $\mathcal{C}$ [see Eq. (6)] simply does not exist, since the density depends as well on the sample history.

We are not aware of a more refined theory that allows one to incorporate such a history. In view of the possible deficiency of this method, and of the approximate nature of the packing model (Ouchiyama-Tanaka theory), we performed numerical simulations using a tool that has been extensively checked over the past 10 years, and that is able to reproduce realistic stress-strain behavior. The very good agreement between the predicted partial pressure (based on our result and Ouchiyama-Tanaka theory, and which does not include any free parameters) and the numerically determined pressures was enough for us to consider the result as valuable. Although we agree that the final predictions cannot be considered as an exact result (it cannot be more exact than the Ouchiyama-Tanaka theory itself), it turns out that the obtained results are quite satisfactory.

The above point is pragmatic, and does not answer the question of why this agreement is so good in a problem where one might not have expected such an approach to be applicable. We think that the key has to reside in the order of magnitude of the effects that are expected. The solid fraction of a granular media with a prescribed granulometry is not unique. However, what is much better defined is the solid fraction after a large shear deformation has been imposed to the system, starting from a loose sample so that localization effects are avoided. It is quite widely accepted that in this case the system reaches the so-called ''critical state,'' which is independent of the sample preparation. The solid fraction of the system at the critical state is dependent on the confining pressure for deformable particles (e.g., for clays), but almost not for stiff particles (e.g., sand) (and when no plastic deformation, or breaking occurs). In this case, the typical reproducibility of the solid fraction is less than 1%. It is within this framework that the Ouchiyama-Tanaka model should be considered. Nevertheless, due to the approximate nature of the model, the agreement with experimentally determined compacities is generally worse than 1% error. Therefore at the level of accuracy of the modeling, the critical state solid fraction can be considered as uniquely defined. Similarly, in the numerical simulations, we performed a first compaction whose aim is to get closer to the critical state, and to erase most of the sensitivity to the initial state, or the preparation conditions. We checked numerically that sample to sample fluctuations were indeed small. On the other hand, as the size ratio of a binary mixture is varied, extremely large changes of solid fraction are expected. This goes well beyond the history dependent effect.

For monosize packings in two dimensions, it is well known that a granular packing of disks has a tendency to crystallize into a regular hexagonal array. A slight perturbation leads to the formation of ''crystals'' of large sizes limited by ''grain boundaries.'' In this case, it appears in our numerical simulations that the density is a rapidly changing function of the size ratio and the small particle volume fraction when the latter approaches either 0 or 1 $(\alpha \neq 1)$. This contrasts with the general case where the density showed little evolution with the particle size ratio (i.e., $\partial\psi/\partial\alpha \approx 0$). We did not investigate this case in great detail because of the very large sensitivity of the results on the system size (number of particles) due to the large size of the ''monocrystals.''

Another case that is also ill behaved concerns large particle size ratio in three dimensions, where small particles can percolate through the pore space of the larger particles, and for low enough concentration in small particles (so that a macroscopic segregation has to take place). It is obvious that in such a case, the mean density of the packing has no physical meaning. This case is, however, amenable to a similar treatment, because the pressure supported by the small particles is simply null. Thus we are again facing an effective problem similar to that of a monosize packing. The critical concentration below which a segregation takes place has been studied in detail in particular by Oger [23].

Numerous studies have shown in the past that segregation of particles according to their size could take place under different conditions (vibration, large steady deformation, heap formed by feeding at a fixed position, etc.) (see, e.g., Ref. [24] for a review). These conditions obviously violate the homogeneity requirement needed to apply the above presented analysis.

V. CONCLUSION

We have shown in this paper that the notion of partial pressure supported by a specific granulometric class can be defined and that it is dependent on granulometric classes. Its value can be related to the dependence of the packing density on the particle diameter. The latter property can be expressed in geometrical terms.

In the particular case of a bimodal distribution, our analysis has shown a significant difference between two and three dimensions, and this point is to be underlined in a context where a number of numerical studies are performed in two dimensions and extrapolated to three. The role of dimensionality is obvious in terms of geometry (e.g., static segregation cannot take place in two dimensions), and the relation between partial pressures and solid fraction underlines that a similar role of dimensionality is to be expected in the correlation between contact forces and particle size.

ACKNOWLEDGMENTS

We thank H. J. Herrmann and S. Luding for their MD computer code, which was used as a basis for the programs used in this article. This work is partly supported by the Groupement de Recherche *Physique des Milieux Hétérogènes Complexes* of the CNRS.

APPENDIX

The density c of the packing as a function of the granulometry is given in Eq. (16). Here, we give the explicit equations used to obtain the differential density $\partial\psi/\partial\alpha$:

$$\frac{\partial\psi}{\partial\alpha}=\frac{1}{D}\frac{\partial H}{\partial\alpha}-\frac{H}{D^2}\frac{\partial D}{\partial\alpha}, \tag{A1}$$

where

$$\frac{\partial H}{\partial\alpha}=3\left[f\bar{x}_1^{\,2}\frac{\partial\bar{x}_1}{\partial\alpha}+(1-f)\bar{x}_2^{\,2}\frac{\partial\bar{x}_2}{\partial\alpha}\right],$$

$$\begin{aligned}\frac{\partial D}{\partial\alpha}&=3(1-f)(\bar{x}_2-1)^2\frac{\partial\bar{x}_2}{\partial\alpha}+\frac{3}{\eta}\\&\quad\times\left[f(\bar{x}_1+1)^2\frac{\partial\bar{x}_1}{\partial\alpha}+(1-f)[(\bar{x}_2+1)^2-(\bar{x}_2-1)^2]\frac{\partial\bar{x}_2}{\partial\alpha}\right]\\&\quad-\frac{1}{\eta^2}[f(\bar{x}_1+1)^3+(1-f)[(\bar{x}_2+1)^3-(\bar{x}_2-1)^3)]\frac{\partial\eta}{\partial\alpha},\end{aligned}$$

$$\frac{\partial\eta}{\partial\alpha}=\frac{\kappa}{B}\left[\frac{\partial A}{\partial\alpha}-\frac{A}{B}\frac{\partial B}{\partial\alpha}\right], \tag{A2}$$

and

$$\begin{aligned}\kappa&=\frac{4(8c_o-1)}{13},\\A&=f(\bar{x}_1+1)^2\left(1-\frac{3}{8}\frac{1}{\bar{x}_1+1}\right)+(1-f)(\bar{x}_2+1)^2\\&\quad\times\left(1-\frac{3}{8}\frac{1}{\bar{x}_2+1}\right),\\\frac{\partial A}{\partial\alpha}&=f\left(2(\bar{x}_1+1)-\frac{3}{8}\right)\frac{\partial\bar{x}_1}{\partial\alpha}+(1-f)\left(2(\bar{x}_2+1)-\frac{3}{8}\right)\frac{\partial\bar{x}_2}{\partial\alpha},\\B&=f\bar{x}_1^{\,3}+(1-f)[\bar{x}_2^{\,3}-(\bar{x}_2-1)^3],\\\frac{\partial B}{\partial\alpha}&=3\left[f\bar{x}_1^{\,2}\frac{\partial\bar{x}_1}{\partial\alpha}+(1-f)[\bar{x}_2^{\,2}-(\bar{x}_2-1)^2]\frac{\partial\bar{x}_2}{\partial\alpha}\right].\end{aligned} \tag{A3}$$

Note

$$\begin{aligned}\frac{\partial\bar{x}_1}{\partial\alpha}&=\bar{x}_2+\alpha\frac{\partial\bar{x}_2}{\partial\alpha},\\\frac{\partial\bar{x}_2}{\partial\alpha}&=-f\bar{x}_2^{\,2}.\end{aligned} \tag{A4}$$

We then deduce the partial pressures $\langle p(x_1)\rangle$ and $\langle p(x_2)\rangle$, and the parameter β from Eqs. (14) and (15), respectively, using the above formula.

[1] G. Schneebeli, C. R. Hebd. Seances Acad. Sci. **243**, 125 (1956).

[2] P. Dantu, in *Proceeding of the 4th International Conference on Soil Mechanics and Foundations Engineering* (Butterworths Scientific Publications, London, 1957), Vol. 1, p. 133.

[3] L. Oger, J. C. Charmet, D. Bideau, and J. P. Troadec, C. R. Acad. Sci., Ser. I: Math. **302**, 277 (1986).

[4] P. Dantu, Ann. Ponts Chaussées, **4**, (1967). A film is available from the ''Laboratoire Central des Ponts et Chaussées,'' Paris.

[5] F. Radjai, M. Jean, J. J. Moreau, and S. Roux, Phys. Rev. Lett. **77**, 274 (1996).

[6] T. Travers, D. Bideau, A. Gervois, and J. C. Messager, J. Phys. A **19**, L1033 (1986).

[7] C. H. Liu, S. R. Nagel, D. A. Schecter, S. N. Coppersmith, S. Majumdar, O. Narayan, and T. A. Witten, Science **269**, 513 (1995).

[8] R. P. Behringer and B. Miller, in *Powders & Grains 97*, edited by R. P. Behringer and J. T. Jenkins (Balkema, Rotterdam, 1997), p. 333.

[9] B. Miller, C. O'Hern, and R. P. Behringer, Phys. Rev. Lett. **77**, 3110 (1996).

[10] S. Ouaguenouni and J. N. Roux, Europhys. Lett. **32**, 449 (1995).

[11] P. Claudin and J. P. Bouchaud, Phys. Rev. Lett. **78**, 231 (1997).

[12] C. Eloy and E. Clément, J. Phys. I **7**, 1541 (1997).

[13] A. S. Helle, K. E. Easterling, and M. F. Ashby, Acta Metall. **33**, 2163 (1985).

[14] O. Tsoungui, D. Vallet, J.-C. Charmet, and S. Roux, C. R. Acad. Sci., Ser. II: Mec. Phys., Chim., Sci. Terre Univers **325**, 457 (1997).
[15] J. A. Dodds, J. Colloid Interface Sci. **77**, 317 (1980).
[16] N. Ouchiyama and T. Tanaka, Ind. Eng. Chem. Fundam. **20**, 66 (1981).
[17] D. Bideau and J. P. Troadec, J. Phys. C **17**, L731 (1984).
[18] J. G. Berryman, Phys. Rev. A **27**, 1053 (1983).
[19] M. P. Allen and D. J. Tildesley, *Computer Simulation of Liquids* (Clarendon Press, Oxford, 1987).
[20] D. Tildesley, in *Computational Physics*, edited by R. D. Kenway and G. S. Pawley (Edinburgh University Press, Edinburgh, 1987).
[21] H. J. Herrmann, in *Disorder and Granular Media*, edited by D. Bideau and A. Hansen (North-Holland, Amsterdam, 1993), p. 305.
[22] S. Luding, Ph.D. thesis, University of Freiburg (1994).
[23] L. Oger, Ph.D. thesis, University of Rennes (1983).
[24] *Disorder and Granular Media*, edited by D. Bideau and A. Hansen (North-Holland, Amsterdam, 1993).